# Architecture of PTCDA molecular structures on a reconstructed InSb(001) surface

Dawid Toton
*Department of Physics of Nanostructures and Nanotechnology, Jagiellonian University, Reymonta 4, PL 30-059, Krakow, Poland and Department of Physics, King's College London, Strand, London, WC2R 2LS, United Kingdom*

Szymon Godlewski, Grzegorz Goryl, and Jacek J. Kolodziej
*Department of Physics of Nanostructures and Nanotechnology, Jagiellonian University, Reymonta 4, PL 30-059, Krakow, Poland*

Lev Kantorovich
*Department of Physics, King's College London, Strand, London, WC2R 2LS, United Kingdom*

Marek Szymonski
*Department of Physics of Nanostructures and Nanotechnology, Jagiellonian University, Reymonta 4, PL 30-059, Krakow, Poland*
(Received 22 February 2011; published 30 June 2011)

An extensive scanning tunneling microscopy (STM) study of adsorption of submonolayer coverages of PTCDA molecules on the $c(8 \times 2)$ reconstructed InSb(001) surface is presented together with *ab initio* density functional theory (DFT) calculations. Our DFT calculations explain the variety of adsorption sites seen on the experimental STM images. In particular, we prove that the molecules are oriented with their long axes along the [110] direction. Calculated STM images of the molecule agree well with the high-resolution STM images obtained at the temperature of 77 K. We find that molecules form four covalent bonds between edge oxygen atoms of the PTCDA and In atoms of the surface. We also study in detail their diffusion mechanism and explain their ability to form experimentally observed chains along the [110] direction.

DOI: 10.1103/PhysRevB.83.235431 PACS number(s): 68.43.−h, 68.43.Bc, 68.43.Fg, 68.43.Hn

## I. INTRODUCTION

In recent years, organic semiconductors deposited on various substrates have attracted a considerable attention due to their applications in new electronic technologies. Up to now, many implementations of organic semiconductors have been developed in a field of light-emitting diodes, fast optical switches, and solar panels, to name just a few (see, for instance, Refs. 1–11 and references therein). The application of single molecules or fabricated nanostructures on surfaces for future computing devices, although being at the very early stage, is also regarded as a promising approach to new conceptual developments in molecular electronics.[12] However, for specific applications, the detailed knowledge of electronic structure of single molecules on substrates as well as of the morphology of both surfaces and substrate/molecule interfaces are required.

Among different organic molecules, a perylene derivative, namely, a perylene-3,4,9,10-tetracarboxylic-3,4,9,10-dianhydride (PTCDA) molecule, is regarded as a model system for planar stacking molecules. The adsorption of PTCDA molecules has been widely studied on metallic,[13–24] semiconducting,[16,25–31] and insulating substrates.[32,33] On chemically inert surfaces [e.g., Au(111)], the molecules usually form ordered assemblies due to the dominance of the intermolecular interactions over the molecule-substrate binding.[24] Usually, the PTCDA films exhibit structures similar to those in the bulk PTCDA crystal [102] plane, forming the so-called herringbone layers.[24,34–36] However on other surfaces where a stronger interaction with the molecules takes place, different structures have been observed as well, such as, e.g., the brick-wall phase.[24,37,38] On highly anisotropic templates, formation of one-dimensional molecular chains has been demonstrated.[39,40] There are also several examples of chemically reactive substrates with a high density of dangling bonds exposed into vacuum that immobilize the molecules and preclude them from forming ordered structures.[29]

Among various semiconductors available, the $A_{\mathrm{III}}$-$B_{\mathrm{V}}$ compounds are of great importance for electronic device technology and the structure of their surfaces has been widely studied. In particular, (001) surfaces frequently used as substrates for molecular beam epitaxy have been examined by various experimental and theoretical techniques.[41] The $c(8 \times 2)$ reconstruction is typical for compounds such as InSb, InAs, and GaAs prepared by ion sputtering or by molecular beam epitaxy (MBE) in $B_{\mathrm{V}}$-deficient conditions followed by annealing. A structural model for surfaces of these compounds (the $\zeta$ model) was proposed by Lee *et al.*[42] and Kumpf *et al.*,[43,44] and was subsequently supported by a few independent theoretical and experimental studies[45–48] and recently was proved to be the ground state under certain experimental conditions.[49,50] According to this model, the surface top bilayer exhibits mostly a $4 \times 1$ symmetry and the $c(8 \times 2)$ superstructure is introduced by $A_{\mathrm{III}}$ atom dimerization in the second bilayer.

The presence of dangling bonds leading to high reactivity of the surface as well as its anisotropy makes the $c(8 \times 2)$ InSb(001) substrate particularly interesting as a template for growing nanostructures. The main characteristic features of this surface are elevated rows of In atoms running along the [110] direction, the so-called In-1 rows.[43,44]

Moreover, the system of PTCDA-InSb combining two important classes of materials, i.e., organic dyes and low band-gap semiconductors exhibiting extremely high carrier mobility may have potential applications in future optoelectronic

 

devices, e.g., light-emitting diodes, photovoltaic detectors, or organic field-effect transistors.

The self-assembly of PTCDA molecules at submonolayer coverages on an anisotropic InSb(001) surface has been investigated previously by means of low-temperature scanning tunneling microscopy[39] (STM) and room-temperature noncontact atomic force microscopy (NC-AFM),[51] revealing formation of molecular chains extending along the surface [110] crystallographic direction. STM and AFM measurements were, however, insufficient to explore in detail the substrate-molecule and molecule-molecule interactions, orientation of individual molecules with respect to the surface features, and the formation of molecular chains. In particular, there has been some controversy concerning the orientation of the adsorbed molecules on the surface. In Ref. 51, three different orientations of molecules were introduced. However, in Ref. 39, it was argued that the molecules are oriented with their longer axis perpendicular to the [110] direction on the basis of high-resolution STM measurements performed at low temperature.

Recently, theoretical studies based on the *ab initio* density functional theory (DFT) calculations were performed for the first time on the InSb(001) surface.[52,53] These calculations supported the model of Kumpf *et al.*[43,44] for this surface and allowed us to identify unequivocally a number of features on the STM images with the help of the atomistic model, including the appearance of the In-1 rows. This information has not been available during the previous studies (mentioned above) of the adsorption of the PTCDA molecules on this surface, so previous interpretations were prone to a speculation to some extent.

The necessity to interpret correctly the observed STM images of PTCDA molecules on the InSb (001) surface in view of the new available experimental and theoretical data, and to explore in detail the binding mechanism of the molecules with the surface as well as the molecular morphology, encouraged us to undertake additional STM studies at both room (RT) and low (77 K) temperatures (LT) of this system and perform corresponding theoretical calculations to interpret available experimental data.

The plan of the paper is as follows: In the next section, experimental setup and results are described in detail. In Sec. III, our theoretical methods are briefly explained and our results are presented, while in the last section, a discussion of the results is given and short conclusions are drawn.

## II. EXPERIMENT

### A. Experimental setup

The whole experiment was carried out in a ultrahigh vacuum (UHV) multichamber system allowing for sample preparation, molecular beam deposition, and surface structure analysis. The temperature of the sample during preparation was controlled by an infrared pyrometer. High-resolution surface structure imaging was performed at RT and LT with the commercially available STM designed by Omicron. The microscope was operated mainly in constant current mode, with the tunneling current varying in the range of 2–500 pA. Electrochemically etched tungsten tips were used as probes. Epi-ready InSb(001) wafers (Kelpin Crystals) were inserted into the UHV chamber and annealed at 700 K for several hours. Subsequently, substrate surface preparation was performed by $Ar^+$ ion beam sputtering with subsequent annealing at 700 K. The sputtering was performed at a beam energy of 700 eV using 45° off-normal incidence and a current density of about 0.5 $\mu A/cm^{-2}$. The sputtering cycles (approximately 30 minutes of duration) were repeated until a clear $c(8 \times 2)$ LEED pattern was observed. The procedure yields InSb(001) surfaces with large atomically flat terraces separated by monolayer steps.[54]

PTCDA molecules were evaporated using the standard effusion cell. During molecule epitaxy, the substrate was kept at RT and no annealing of the sample at elevated temperatures has been applied. The deposition process was performed in the $10^{-10}$-mbar pressure range at a rate of 0.3 ML/min as calibrated by a quartz-crystal microbalance. For image processing and data analysis, WSxM software has been applied.[55]

### B. STM images of the PTCDA adsorbed on the surface

A typical STM image acquired at RT of a rather large area of the surface is shown in Fig. 1(a). One can clearly see chains of different lengths composed of rectangular features aligned along the [110] direction. These features are seen to occupy two possible positions in the direction across the chain: In ≃59% of cases, the neighboring molecules are arranged head-to-tail along the chain, however, in ≃41% of cases, the

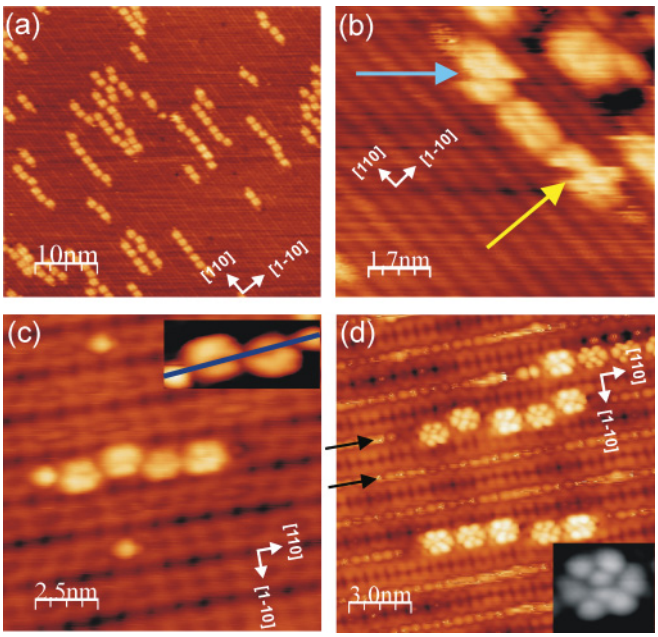


FIG. 1. (Color online) Typical filled-state STM images of the PTCDA chains on the InSb(001) surface. (a) RT image, area 40 × 40 nm ($I_t = 2$ pA, $V_t = -2.0$ V); (b) jumps along (yellow arrow) and across (blue arrow) the chain, RT ($I_t = 2$ pA, $V_t = -2.0$ V); (c) LT (77 K) image ($I_t = 10$ pA, $V_t = -1.0$V); the inset exposes asymmetries of appearance of the chain with respect to the In-1 row, which is marked with blue line. (d) LT high-resolution image, area 14 × 14 nm ($I_t = 500$ pA, $V_t = -0.5$V); an inset presents a magnified single-molecule high-resolution STM image; black arrows point to the In-1 rows of the substrate.

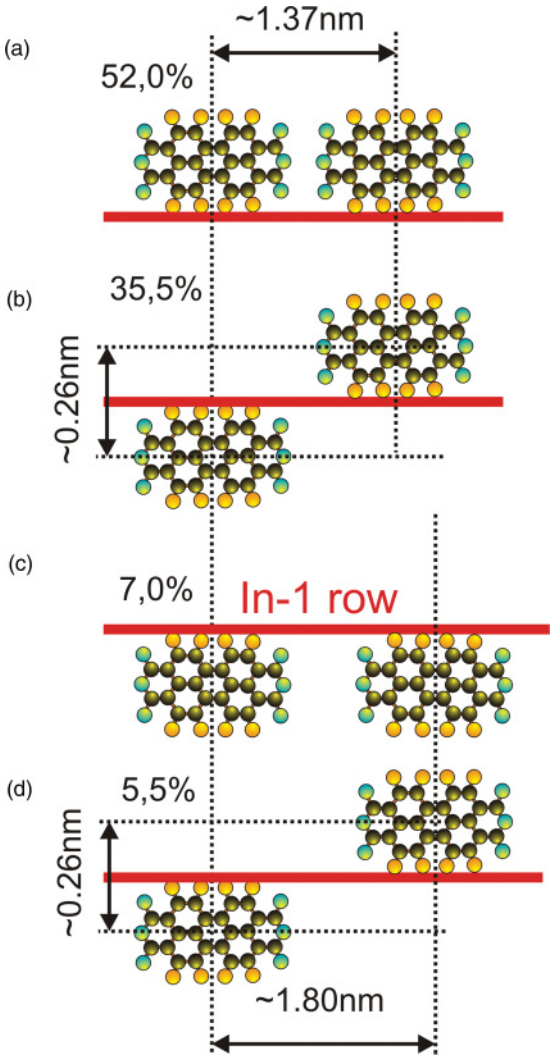


FIG. 2. (Color online) Schematic view of four possible arrangements of neighboring molecules along the chain, either head-to-tail [(a), (c)] or shifted [(b), (d)]. The position of the In-1 row (the bold red horizontal line), distances between the molecules in the direction along and across the chain, measured between the centers of the rectangular features and the percentage of all geometries as observed in our STM images, are also indicated.

molecules are somewhat displaced (the average displacement obtained by considering about 20 molecules was found to be 0.26 ± 0.02 nm); this is schematically shown in Fig. 2.[39] Moreover, a detailed analysis also revealed that most often (in ≃87.5% of cases as estimated using around 200 molecules) the adjacent molecules are separated along the chains by 1.37 ± 0.08 nm (which is close to $3a$, where $a = 0.458$ nm is the distance between neighboring In-1 atoms along the same row), while in a relatively small number of cases (≃12.5%), the distances between the neighboring molecules in the chains are somewhat larger (1.80 ± 0.07 nm, which is close to $4a$). Sometimes when scanning at RT, switching of the molecules between these possible positions, both along and across the chain, can be induced by the STM tip as shown in Fig. 1(b). We never observed such events when scanning at LT.

A close view of the molecules in the chain taken by STM is shown in Fig. 1, demonstrating some submolecular resolution for the PTCDA molecules. Both in LT [Fig. 1(c)] and RT STM [Figs. 1(a) and 1(b)] measurements, each molecule is typically represented by two elongated lobes of different sizes.[39] The lobes are aligned along the In-1 direction, with the smaller lobe being closer to the In-1 row, as Fig. 1(c) demonstrates. The apparent difference between the lengths of the two lobes depends on the imaging conditions. That difference has been analyzed statistically for the conditions used during the scan shown in Fig. 1(a), and the obtained average ratio of the lengths along the [110] direction (estimated from the images of around 20 molecules) equals 1.13 ± 0.09. Note that a much better submolecular resolution has been achieved when performing high-resolution STM imaging at LT (with significantly higher tunneling current) as can be seen in Fig. 1(d), where, instead of each of the two lobes, we observe five features arranged in two lines with two and three features in each (see the inset).

Another remarkable feature that can clearly be noticed in the discussed STM images is related to bright spots appearing at the ends of most chains exactly above the In-1 row (i.e., next to the smaller lobe). This feature was observed with almost equal success for both LT and RT conditions. Moreover, we find that, in most cases (64%), both ends of the chains contain bright spots; however, in some cases (31.5%), we observed only a single spot or none (4.5%), as can be seen in Fig. 3. An explanation for this phenomenon will be proposed below based on our DFT calculations.

## III. THEORETICAL

### A. Theoretical methods

In our calculations, we used an *ab initio* SIESTA method,[56] which is based on periodic boundary conditions and the method of pseudopotentials. The setup of our calculations is similar to the ones used previously.[52,53] We used the Perdew-Burke-Ernzerhof (PBE) density functional[57] and the

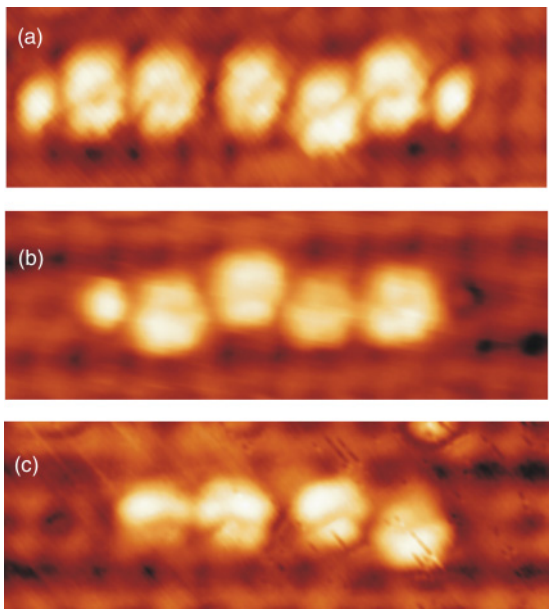


FIG. 3. (Color online) Typical LT-STM (77 K) images of PTCDA chains with (a) two, (b) one, and no bright spots at the ends ($I_t$ = 10 pA, $V_t = -1.0$ V).

double-$\zeta$-polarized (DZP) numerical basis set corresponding to the confinement energy of 10 meV. All geometries were relaxed until forces on atoms were less than 0.04 eV/Å. Two bottom layers of the slab, together with the terminating hydrogen atoms, were fixed, and all other atoms were fully allowed to relax. In most of our calculations, we used a single $\Gamma$ ($\mathbf{k} = 0$) point in the **k**-point sampling due to considerable sizes of the cells used.

While discussing energetics of adsorption of molecules on the surface, a number of useful energies are introduced. The deformation energy $E_{\mathrm{def}}^{X}$ of a part $X$ of the system (either the molecule or surface) is obtained by calculating the difference of the total energies of the part $X$ in two geometries: (i) as relaxed in vacuum and (ii) as found relaxed in the full system and extracted afterwards. Obviously, this energy is always positive and shows the energy lost by the part $X$ while forming the combined system. $E_{\mathrm{int}}$ is the interaction energy related to, e.g., formation of a chemical bonds between molecule and surface. It is always negative if the final system is stable. Finally, we define the adsorption (binding) energy $E_{\mathrm{ads}}$, which is a sum of the interaction and deformation energies for all parts of the entire system. In our calculations, the adsorption and interaction energies include the basis-set superposition error (BSSE) correction, which is related to the fact that the basis set used in SIESTA is localized on atoms and, hence, different basis sets are used for different individual parts and the combined system when calculating these energies. We used the standard counterpoise method to calculate this correction.[58]

When calculating STM images, we used the Tersoff-Hamann approximation[59] whereby the local electronic density of states (LDOS) serves as an approximation for the STM signal. Whereas the Tersoff-Hamann approximation is an approximate method applicable only for small bias voltages and not very close tip-surface separations, it is sufficient in most cases where qualitative comparison of simulated and experimental images is essential for structure recognition.

### B. Results of calculations

We placed the molecule at over 20 various configurations above the surface, which varied both in the molecule lateral position and orientation, and then relaxed the entire structure. Most of the calculations were done using the $4 \times 4$ surface cell consisting of two $4 \times 2$ cells (see Ref. 52) to reduce the cost of the calculations; however, in the cases of biggest adsorption energies [Figs. 4(a)–4(c)], a bigger $8 \times 4$ cell was used. A selection of the obtained geometries is shown schematically (the top view) in Fig. 4. The corresponding adsorption energies (in eV) are reported in Table I together with other relevant energies as discussed in Sec. III A.

As is seen from Table I, the BSSE energies are in all cases significant. It follows from our calculations that the most energetically favorable geometries correspond to the molecules oriented with their long axis along the [110] direction with one of their sides above the In-1 row [the geometries (a)–(c) in Fig. 4].

In fact, a more detailed analysis shows that the most stable adsorption geometries are due to formation of four chemical bonds between corner oxygen atoms of the PTCDA and In atoms of the surface, and when one side of the PTCDA is bound to two In-1 atoms, while the other side is bound to atoms of the row formed by In-4 and In-5 atoms. Since these conditions can be satisfied when the either side of the molecule is bound to the In-1 atoms and because of the symmetry of the surface, it is clear that, for every geometry with the molecule on one side of the In-1 row, there is an equivalent one on the other.

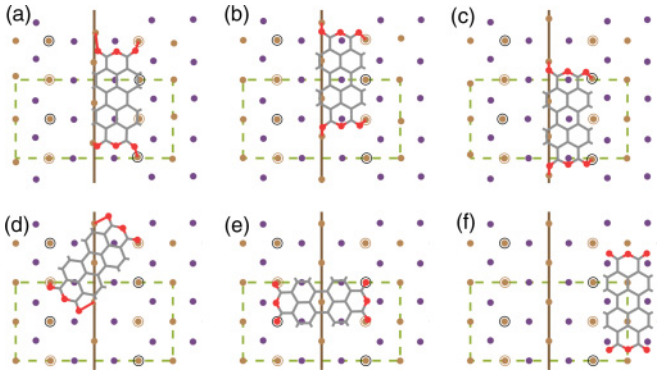


FIG. 4. (Color online) Schematics (based on the actual DFT relaxed geometries) of a number of stable adsorption configurations of the PTCDA molecule on the InSb(001) surface. The In-1 row atoms, as well as the In-4 and In-5 atoms, and other species are distinguished using the following color scheme: red, oxygen; violet, antimony; brown, indium. In-4 and In-5 atoms are marked with brown and black rings, respectively. The brown line indicates the In-1 row of atoms. The dashed rectangle is of the $4 \times 2$ size and corresponds to the half of the surface elementary cell; it was used to build the $4 \times 4$ surface slab used in these simulations (for details see text).

However, we find that the situation is even more complex. Because of a very small energy barrier of 0.08 eV (Ref. 53) for the In-1 atom to move along the [110] direction, and the fact that the aromatic core of the PTCDA molecule may bend with relatively small deformation energies (as shown in Fig. 5 and Table I), we suggest that more configurations of the PTCDA satisfying the above-mentioned constraints may be possible. In a way, there is a certain flexibility for the PTCDA molecule to find its position along the In-1 row depending on the available In-1, In-4, and In-5 atoms and the positions of the neighboring PTCDA molecules.

DFT calculations reveal the amount of charge transferred from the surface to the molecule: in the cases of the

TABLE I. $E_{\mathrm{ads}}$ of the PTCDA molecule on the InSb(001) surface for the selection of stable geometries shown in Fig. 4. $E_{\mathrm{int}}$ and $E_{\mathrm{def}}^{X}$ are the interaction and deformation energies (for both $X$ being the surface and the molecule), while $E_{\mathrm{BSSE}}$ is the corresponding BSSE correction. All energies reported are in eV.

| Case | $E_{\mathrm{int}}$ | $E_{\mathrm{def}}^{\mathrm{InSb}}$ | $E_{\mathrm{def}}^{\mathrm{PTCDA}}$ | $E_{\mathrm{BSSE}}$ | $E_{\mathrm{ads}}$ |
|---|---|---|---|---|---|
| a | −3.73 | −0.02 | 0.58 | 0.49 | −3.18 |
| b | −3.76 | 0.08 | 0.66 | 0.47 | −3.01 |
| c | −3.85 | 0.03 | 0.72 | 0.47 | −3.10 |
| d | −3.52 | 0.29 | 0.84 | 0.46 | −2.39 |
| e | −3.51 | 0.43 | 1.00 | 0.45 | −2.08 |
| f | −1.01 | 0.04 | 0.08 | 0.26 | −0.89 |

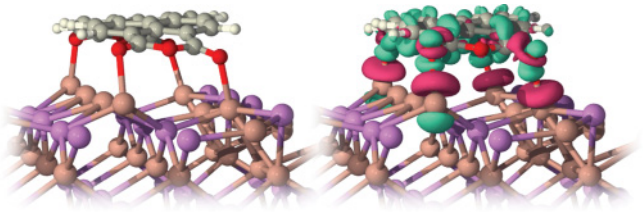

FIG. 5. (Color online) Geometry of the configuration shown in Fig. 4(b) (left) and the corresponding charge-density difference plot (right). The red and green colors correspond to depletion and excess of the electron density, respectively, as compared to the isolated molecule and surface, with the contour levels of −0.017 and +0.017 electron/Å$^3$.

aforementioned most favorable geometries, it ranges from 2.0 to 2.3$e$, and PTCDA is charged negatively. These numbers result from the following division of simulation cell space into two integration volumes: a given point is included in the first volume if the atom that is closest to it belongs to the molecule.

The plot of the electron density difference between the whole system and the densities of the individual molecule and the surface (in the geometry of the combined system) shown in Fig. 5(b) demonstrates the formation of four covalent bonds between the oxygens of PTCDA and In atoms. In fact, there is a direct correlation between the interaction energies and the proximity of involved In atoms to the corresponding oxygen atoms of the PTCDA. This is reported in Fig. 6 for all geometries considered in this study where the dependence of $E_{\text{int}}$ on the sum of four distances calculated between the four O-In pairs is plotted. Note that the corresponding In atom for each corner O atom of the molecule was chosen by the smallest possible distance. One can clearly see that the largest interaction energies appear when the average O-In distance is no longer than about 0.26 nm, which clearly corresponds to the formation of O-In covalent bonding exemplified by the bonds shown in Fig. 5(b).

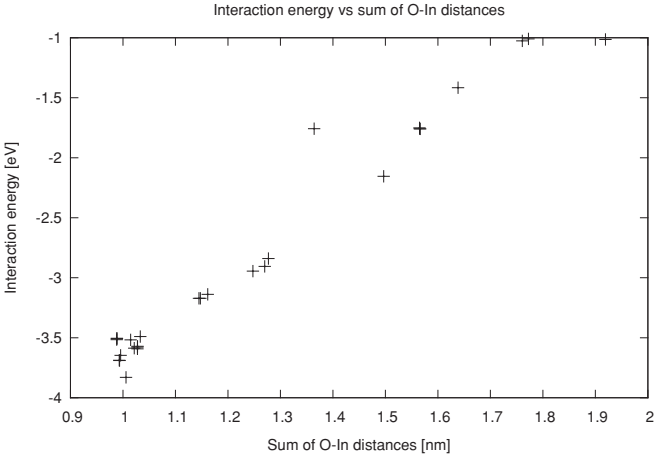


FIG. 6. Interaction energy $E_{\text{int}}$ (in eV) of all considered DFT relaxed geometries of the PTCDA molecule on the InSb(001) surface plotted as a function of a sum of four distances between molecule corner O atoms and nearest In atoms of the surface (in Å).

Each O-In pair brings approximately extra 0.9 eV to the $E_{\text{int}}$. This enables the molecule to fit to the surface geometry in such a way that the resulting deformation (e.g., bending) would not be too costly.

In all calculations presented so far, we assumed 100% occupancy of the In-1 sites. As it is known from detailed experimental studies,[44,53] the In-1 row is only around 57% occupied by In atoms. Therefore, for the sake of completeness, we performed additional calculations with PTCDA deposited on surface models with 33% and 50% of In-1 sites left vacant. The resulting optimized geometries reveal no significant differences when compared with the previously considered models assumed to have 100% In-1 occupation.

Several cases were considered with vacancies arranged in different ways. Whenever there are four In atoms available in proximity to the O atoms of the PTCDA, the molecule forms four covalent bonds with the In-1 atoms with the adsorption energy being almost identical to that found above in the case of the fully occupied In-1 row. For other distributions of vacancies, formation of only three O-In bonds is possible, leading to lowering of the binding energy by approximately 0.4 eV per molecule. It clearly shows that it is much more energetically favorable for the molecules to form all four covalent bonds with the surface In atoms. Due to high mobility of the In atoms on the In-1 rows and low PTCDA coverages, it seems clear that, for any molecule, there will always be four In atoms available to bind to. Therefore, we believe that performing calculations with fully occupied In-1 rows would not affect our main conclusions. Hence, we restrict ourselves to that case in what follows.

The calculated STM image of the molecule on the surface in configuration (a) shown in Fig. 4 is given in the right panels of Fig. 7. To demonstrate the expected change in the STM image due to two possible equivalent positions of the molecule with respect to the In-1 row, as discussed above, we show the images of these structures together as they would appear in the chain. The corresponding schematics of the two configurations are also shown on the left for convenience. In the middle of each calculated image of the molecule, one can see a ditch in the isosurface that appears as a dark vertical line. It divides each image in two halves. The one that is further away from the In-1 row is more prominent. Each of the halves has an internal structure showing two larger external lobes and three smaller internal ones. These results perfectly agree with the experimental high resolution LT images of the molecule reported in Sec. II B as shown in the inset in Fig. 1(d). If the imaging conditions are worse, the internal structure of the molecular image is partially smeared out, and only two large lobes extended along the [110] direction remain visible, as shown in Figs. 1(a), 1(b), and 1(c).

To understand the formation of the PTCDA chains, we performed additional calculations in which we considered diffusion of a single molecule along the [110] and [1$\bar{1}$0] directions. In these calculations we moved the molecule in small steps along the given direction **r** and relaxed the system at each position. In particular, one of the carbon atoms of the perylene core of the PTCDA was forced to move along **r** and allowed to relax only within the plane perpendicular to **r**. All other atoms, apart from the bottom layers of the surface slab, moved freely.

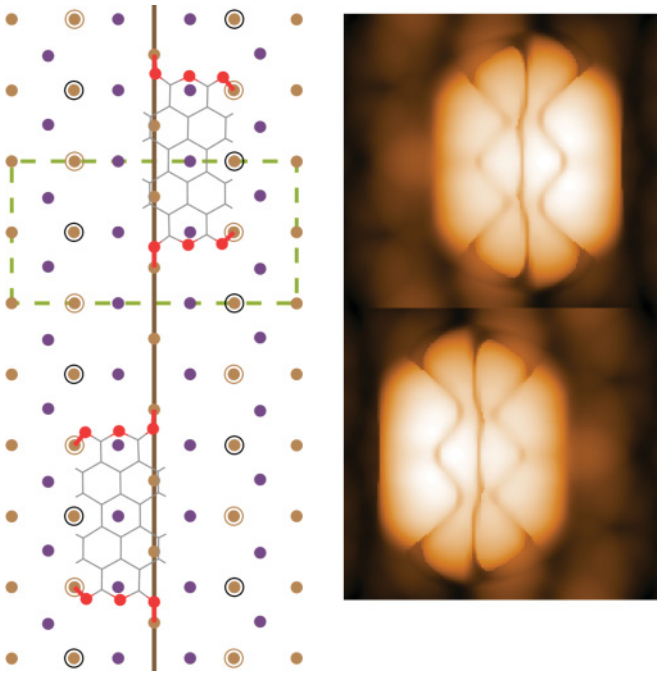

FIG. 7. (Color online) Calculated STM images of the configuration (a) in Fig. 4 (right panels) shown for two possible positions of the molecule (left panels) with respect to the In-1 row indicated by the solid line ($V_t = -1.0$ V). The In-1 rows in both STM images are aligned with each other for convenience.

We find that the diffusion path in the direction $[1\bar{1}0]$ perpendicular to the In-1 row has a complicated structure (not shown); however, a general tendency is to increase the energy considerably as the molecule moves away from its most favorable positions near the In-1 row. Initially, there are barriers of $\simeq$0.5 eV to shift the molecule away from the In-1 row by $\simeq$3 and $\simeq$6 Å, however, further displacement of the molecule requires overcoming the energy barrier larger than 1 eV. At the same time, we find that diffusion of the molecule along the In-1 row requires overcoming much smaller barriers of the order of 0.3 eV. This is due to the fact that when the molecule moves along the In-1 row, the O-In bonds are exchanged from the current In atom to the next one along the path not all at the same time, but one by one, which reduces the energy barrier along this direction. These data, as well as the fact that the molecule adsorbs more favorably with one of its longer sides on the In-1 row, help to explain the formation of one-dimensional chains.

The last thing that is left to explain is the appearance of bright spots at the edges of the observed PTCDA chains, as seen, e.g., in Fig. 3. While performing diffusion calculations of the molecule, we discovered that additional lowering of the total energy by $\simeq$0.1 eV is achieved if the In-1 atom next to the one already engaged in the bonding to the molecule is lifted and pulled close to the latter, as shown in Fig. 8(a). The simulated STM image of this geometry, shown in Fig. 8(b), clearly demonstrates that this lifted atom appears as a bright spot next to the less pronounced lobe representing the part of the molecule above the In-1 row. These findings are in good agreement with the bright spots found at the ends of chains as observed in our STM images.

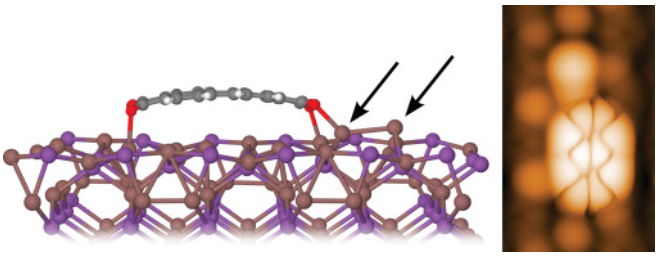

FIG. 8. (Color online) The relaxed geometry (a) and the corresponding calculated STM image (b) of the PTCDA molecule with one of the nearest In-1 atoms lifted close to the one already involved in the O-In covalent bond (both atoms are indicated by the arrows).

An alternative scenario concerning the origin of the bright spots would be purely electronic, i.e., due to accumulation of the electron density at the edges of PTCDA chains. Note, however, that explanation is highly unlikely as we have not observed such effects in our calculations and, therefore, we conclude that only the surface distortion at the ends of PTCDA chains can explain the presence of bright spots observed experimentally.

## IV. DISCUSSION AND CONCLUSIONS

We have considered in detail, using both experiment and theory, the PTCDA/InSb(001) $c(8 \times 2)$ adsorption system. We find that PTCDA molecules are adsorbed on the surface with large adsorption energies by formation of covalent bonds between its four corner oxygen atoms and available In atoms of the surface. Because of the mostly fixed positions of the oxygen atoms in the PTCDA molecule and of the In-4,5 atoms on the surface, only certain adsorption geometries are possible. The most favorable configurations were found when two of the oxygen atoms at one long side of the molecule bind directly to the In atoms of the In-1 row (seen as the bright thin line in the STM images). The simulated STM images agree well with the HR experimental images, and this fact serves as an additional confirmation of our atomistic interpretation of the STM images.

The theoretical results presented here explain why the chains observed in our experiments are aligned along the [110] direction. Moreover, because oxygen atoms from either side of the PTCDA may bind to the In-1 atoms, we also managed to explain why, within the chains, molecules may appear on either side of the line of bright spots assigned to In-1 atoms. According to acquired statistics presented in Fig. 2, there is only a very small preference for the molecules within the chains to stay in the head-to-tail configuration to their neighbors (59%). We speculate that the small preference of the head-to-tail configurations may be explained by some rather small energy penalty due to a shift of the molecule across the chain.

We have also successfully explained the appearance of bright spots at the ends of chains in the experimental images, which we attributed to lifted In-1 atoms. We believe that the lifting of the In-1 atom would only be possible if the molecule is at the end of the chain as when two molecules are close to each other within the chain, even at the distance of 4*a*

(see Sec. II B), there would be no free In-1 atoms between them. That is why the bright spots appear only at the ends of the chains. Since the energy difference between the two states (lifted and not lifted In-1 atom) is not very large and there must be an energy barrier separating them (not calculated here), not all chains have these edge atoms, or may have only one as we have observed in our experiments.

Our main conclusions are drawn from the calculations performed within the models that assume the 100% occupancy of the In-1 sites. It is known from experimental investigations[44,53] that the In-1 row is only around 57% occupied by In atoms.

However, as discussed at the end of Sec. III B, the simplifying assumption of full In-1 occupancy will not change our main qualitative conclusions concerning the most favorable lattice sites, orientation, and location of the adsorbed PTCDA molecules, their STM image, and the conclusion we made concerning the bright spots at the ends of chains. However, our calculated barriers for the PTCDA diffusion may be affected by lower occupancy of the In-1 row. We also believe that this lower occupancy of the In-1 rows is essential in explaining the reasons behind the kinetics of PTCDA chain formation. We plan to investigate these latter points in a separate study.

Thus, our theoretical results for the PTCDA adsorption on the InSb(001) surface agree with experiments on all essential points: (i) chains of molecules are formed along the [110] direction; (ii) there are two possible positions of the molecules across the chains with respect to the In-1 row; (iii) at RT, molecules appear in the STM images with two lobes elongated along the [110] direction; (iv) one of the lobes is smaller than the other, and the smaller lobe is positioned closer to the In-1 row; (v) at LT, the molecules appear in the STM images with a substructure of ten bright features (five for each of the lobes); and (vi) bright spots are observed at the ends of the chains. This excellent agreement proves without doubt that the molecules on the surface are oriented with their long axes along the [110] direction, opposite to the conclusion reached in the previous study.[39] We therefore also have a strong confirmation that the lines of bright spots in the experimental images of the bare InSb(001) surface running in the [110] direction correspond indeed to the topmost In atoms (the In-1 row) as was inferred previously.[52,53]

There are many studies in which large organic molecules were considered on *simple* metal, semiconducting, and insulating surfaces. In some of these studies, both experiment and theory were used to understand the molecular assembly. However, this paper is a rather rare example of a comprehensive theoretical and experimental investigation related to the adsorption of large planar organic molecules, such as PTCDA, on a very complicated reconstructed semiconducting surface, such as InSb(001).

## ACKNOWLEDGMENTS

This work was supported by the 6th Framework EU Programme PICO-inside, Project No. FP6-15847, and the 7th Framework EU Programme within the Coordination Action Nano-scale ICT Devices and Systems, NanoICT, Contract No. 216165, and also by the Polish Ministry of Science and Higher Education under Contracts No. 1802/B/H03/2010/38 and No. 1044/B/H03/2009/36. S.G. would like to acknowledge support received from the Foundation for Polish Science within START program (2010 and 2011). Via our membership of the UK's HPC Materials Chemistry Consortium, which is funded by EPSRC (EP/F067496), this work made use of the facilities of HECToR, the UK's national high-performance computing service, which is provided by UoE HPCx Ltd at the University of Edinburgh, Cray Inc. and NAG Ltd, and funded by the Office of Science and Technology through EPSRC's High End Computing Programme. D.T. would also like to acknowledge a partial financial support from the Thomas Young Centre (TYC), London.

[1] S. R. Forrest, Nature (London) **428**, 911 (2004).
[2] M. Gratzel, Nature (London) **414**, 338 (2001).
[3] S. R. Forrest, Chem. Rev. **97**, 1793 (1997).
[4] N. Peyghambarian and R. A. Norwood, Opt. Photonics News **16**, 28 (2005).
[5] H. Ishii, K. Sugiyama, E. Ito, and K. Seki, Adv. Mater. **11**, 605 (1999).
[6] N. Koch, ChemPhysChem **8**, 1438 (2007).
[7] S. J. Tans, A. R. M. Verschueren, and C. Dekker, Nature (London) **393**, 49 (1998).
[8] J. Chen, M. A. Reed, A. M. Rawlett, and J. M. Tour, Science **286**, 1550 (1999).
[9] Z. J. Donhauser, B. A. Mantooth, K. F. Kelly, L. A. Bumm, J. D. Monnell, J. J. Stapleton, D. W. Price, A. M. Rawlett, D. L. Allara, J. M. Tour, and P. S. Weiss, Science **292**, 2303 (2001).
[10] M. Magoga and C. Joachim, Phys. Rev. B **56**, 4722 (1997).
[11] S. Ami, M. Hliwa, and C. Joachim, Chem. Phys. Lett. **367**, 662 (2003).
[12] C. Joachim, J. K. Gimzewski, and A. Aviram, Nature (London) **408**, 541 (2000).
[13] M. Stöhr, M. Gabriel, and R. Möller, Europhys. Lett. **59**, 423 (2002).
[14] C. Loppacher, U. Zerweck, L. M. Eng, S. Gemming, G. Seifert, C. Olbrich, K. Morawetz, and M. Schreiber, Nanotechnology **17**, 1568 (2006).
[15] L. Romaner, D. Nabok, P. Puschnig, E. Zojer, and C. Ambrosch-Draxl, New J. Phys. **11**, 053010 (2009).
[16] S. Duhm, A. Gerlach, I. Salzmann, B. Bröker, R. Johnson, F. Schreiber, and N. Koch, Org. Electron. **9**, 111 (2008).
[17] S. Henze, O. Bauer, T.-L. Lee, M. Sokolowski, and F. Tautz, Surf. Sci. **601**, 1566 (2007).
[18] A. Kraft, R. Temirov, S. K. M. Henze, S. Soubatch, M. Rohlfing, and F. S. Tautz, Phys. Rev. B **74**, 041402 (2006).
[19] M. Rohlfing, R. Temirov, and F. S. Tautz, Phys. Rev. B **76**, 115421 (2007).
[20] M. Schneider, E. Umbach, and M. Sokolowski, Chem. Phys. **325**, 185 (2006).

[21]M. Stöhr, M. Gabriel, and R. Möller, Surf. Sci. **507-510**, 330 (2002).
[22]R. Temirov, S. Soubatch, A. Luican, and F. S. Tautz, Nature (London) **444**, 350 (2006).
[23]M. V. Tiba, O. Kurnosikov, C. F. J. Flipse, B. Koopmans, H. J. M. Swagten, J. T. Kohlhepp, and W. J. M. de Jonge, Surf. Sci. **498**, 161 (2002).
[24]F. Tautz, Prog. Surf. Sci. **82**, 479 (2007).
[25]D. R. T. Zahn, G. N. Gavrila, and G. Salvan, Chem. Rev. **107**, 1161 (2007).
[26]C. Kendrick and A. Kahn, J. Cryst. Growth **181**, 181 (1997).
[27]C. Kendrick and A. Kahn, Appl. Surf. Sci. **123-124**, 405 (1998).
[28]C. Kendrick and A. Kahn, Surf. Rev. Lett. **5**, 289 (1998).
[29]Y. Hirose, S. R. Forrest, and A. Kahn, Phys. Rev. B **52**, 14040 (1995).
[30]T. Soubiron, F. Vaurette, J. Nys, B. Grandidier, X. Wallart, and D. Stiévenard, Surf. Sci. **581**, 178 (2005).
[31]P. J. Unwin, D. Onoufriou, and T. S. Jones, Surf. Sci. **547**, 45 (2003).
[32]T. Kunstmann, A. Schlarb, M. Fendrich, T. Wagner, R. Möller, and R. Hoffmann, Phys. Rev. B **71**, 121403 (2005).
[33]S. A. Burke, W. Ji, J. M. Mativetsky, J. M. Topple, S. Fostner, H.-J. Gao, H. Guo, and P. Grütter, Phys. Rev. Lett. **100**, 186104 (2008).
[34]S. Mannsfeld, M. Toerker, T. Schmitz-Hübsch, F. Sellam, T. Fritz, and K. Leo, Org. Electron. **2**, 121 (2001).
[35]M. Mura, X. Sun, F. Silly, H. T. Jonkman, G. A. D. Briggs, M. R. Castell, and L. N. Kantorovich, Phys. Rev. B **81**, 195412 (2010).
[36]I. Chizhov, A. Kahn, and G. Scoles, J. Cryst. Growth **208**, 449 (2000).
[37]M. Böhringer, W. D. Schneider, K. Glöckler, E. Umbach, and R. Berndt, Surf. Sci. **419**, L95 (1998).
[38]K. Glöckler, C. Seidel, A. Soukopp, M. Sokolowski, E. Umbach, M. Böhringer, R. Berndt, and W. D. Schneider, Surf. Sci. **405**, 1 (1998).
[39]G. Goryl, S. Godlewski, J. J. Kolodziej, and M. Szymonski, Nanotechnology **19**, 185708 (2008).
[40]A. Tekiel, S. Godlewski, J. Budzioch, and M. Szymonski, Nanotechnology **19**, 495304 (2008).
[41]M. Jung, U. Baston, G. Schnitzler, M. Kaiser, J. Papst, T. Porwol, H. J. Freund, and E. Umbach, J. Mol. Struct. **293**, 239 (1993).
[42]S.-H. Lee, W. Moritz, and M. Scheffler, Phys. Rev. Lett. **85**, 3890 (2000).
[43]C. Kumpf, D. Smilgies, E. Landemark, M. Nielsen, R. Feidenhans'l, O. Bunk, J. H. Zeysing, Y. Su, R. L. Johnson, L. Cao, J. Zegenhagen, B. O. Fimland, L. D. Marks, and D. Ellis, Phys. Rev. B **64**, 075307 (2001).
[44]C. Kumpf, L. D. Marks, D. Ellis, D. Smilgies, E. Landemark, M. Nielsen, R. Feidenhans'l, J. Zegenhagen, O. Bunk, J. H. Zeysing, Y. Su, and R. L. Johnson, Phys. Rev. Lett. **86**, 3586 (2001).
[45]D. Paget, Y. Garreau, M. Sauvage, P. Chiaradia, R. Pinchaux, and W. G. Schmidt, Phys. Rev. B **64**, 161305 (2001).
[46]T. D. Mishima, N. Naruse, S. P. Cho, T. Kadohira, and T. Osaka, Phys. Rev. Lett. **89**, 276105 (2002).
[47]J. J. Kolodziej, B. Such, and M. Szymonski, Phys. Rev. B **71**, 165419 (2005).
[48]J. J. Kolodziej, B. Such, M. Szymonski, and F. Krok, Phys. Rev. Lett. **90**, 226101 (2003).
[49]P. Laukkanen, M. P. J. Punkkinen, N. Räsänen, M. Ahola Tuomi, M. Kuzmin, J. Lång, J. Sadowski, J. Adell, R. E. Perälä, M. Ropo, K. Kokko, L. Vitos, B. Johansson, M. Pessa, and I. J. Väyrynen, Phys. Rev. B **81**, 035310 (2010).
[50]J. J. K. Lång, M. P. J. Punkkinen, P. Laukkanen, M. Kuzmin, V. Tuominen, M. Pessa, M. Guina, I. J. Väyrynen, K. Kokko, B. Johansson, and L. Vitos, Phys. Rev. B **81**, 245305 (2010).
[51]J. J. Kolodziej, M. Goryl, J. Konior, F. Krok, and M. Szymonski, Nanotechnology **18**, 135302 (2007).
[52]D. Toton, J. He, G. Goryl, J. J. Kolodziej, S. Godlewski, L. Kantorovich, and M. Szymonski, J. Phys. Condens. Matter **22**, 265001 (2010).
[53]G. Goryl, D. Toton, N. Tomaszewska, J. S. Prauzner-Bechcicki, L. Walczak, A. Tejeda, A. Taleb Ibrahimi, L. Kantorovich, E. G. Michel, and J. J. Kolodziej, Phys. Rev. B **82**, 165311 (2010).
[54]J. J. Kolodziej, B. Such, M. Goryl, F. Krok, P. Piatkowski, and M. Szymonski, Appl. Surf. Sci. **252**, 7614 (2006).
[55] I. Horcas, R. Fernandez, J. M. Gomez-Rodriguez, J. Colchero, J. Gomez-Herrero, and A. M. Baro, Rev. Sci. Instrum. **78**, 013705 (2007).
[56]J. M. Soler, E. Artacho, J. D. Gale, A. García, J. Junquera, P. Ordejón, and D. Sánchez-Portal, J. Phys. Condens. Matter **14**, 2745 (2002).
[57]J. P. Perdew, K. Burke, and M. Ernzerhof, Phys. Rev. Lett. **77**, 3865 (1996).
[58]S. Boys and F. Bernardi, Mol. Phys. **19**, 553 (1970).
[59]J. Tersoff and D. R. Hamann, Phys. Rev. B **31**, 805 (1985).